REPORT

Hydrogeology and groundwater management in a coastal granitic area with steep slopes in Galicia (Spain)

Acacia Naves[1] · Javier Samper[1] · Bruno Pisani[1] · Alba Mon[1] · Jorge Dafonte[2] · Luis Montenegro[1] · Aitor García-Tomillo[3]

Abstract

Groundwater availability, management and protection are great challenges for the sustainability of groundwater resources in the scattered rural areas of the Atlantic regions of Europe where groundwater is the only option for water supply. This report presents a hydrogeological study of the coastal granitic area of Oia in northwestern Spain, which has unique geomorphological and hydrogeological features with steep slopes favoring the erosion of the weathered granite. The hydrogeological conceptual model of the study area includes: (1) the regolith layer, which is present only in the flat summit of the mountains; (2) the slope debris and the colluvial deposits, which are present in the intermediate and lowest parts of the hillside; (3) the marine terrace; and (4) the underlying fractured granite. Groundwater recharge from rainfall infiltration varies spatially due to variations in terrain slope, geology and land use. The mean annual recharge estimated with a hydrological water balance model ranges from 75 mm in the steepest zone to 135 mm in the lowest flat areas. Groundwater flows mostly through the regolith and the detrital formations, which have the largest hydraulic conductivities. Groundwater discharges in seepage areas, springs, along the main creeks and into the sea. The conceptual hydrogeological model has been implemented in a groundwater flow model, which later has been used to select the best pumping scenario. Model results show that the future water needs for domestic and tourist water supply can be safely provided with eight pumping wells with a maximum pumping rate of 700 m^3/day.

Keywords Igneous rocks · Numerical modelling · Groundwater recharge/water budget · Spain · Water supply

Introduction

Well failure and low well yields (<20 m^3/day) are common in hard rocks aquifers (Taylor and Howard 2000; Courtois et al. 2009). However, these types of aquifers are well suited for the water supply of scattered populations where total demand is low in comparison to more populous areas. Groundwater resources are commonly found in the first tens of meters below the ground surface (Detay et al. 1989). Their geometry, hydraulic conductivity and storativity depend mainly on the weathering of the parent rock and stripping (colluvial and fluvial erosion; Taylor and Howard 2000; Wyns et al. 2004). A typical weathering profile includes two main stratiform layers subparallel to the paleo-surface contemporaneous of the weathering processes having specific hydrodynamic properties (Chilton and Smith-Carington 1984; Chilton and Foster 1995; Wyns et al. 1999, 2004; Krásný 2002; Maréchal et al. 2004, 2006; Lubczynski and Gurwin 2005; Dewandel et al. 2006; Krásný and Sharp 2007). From top to bottom, the weathering profile includes: (1) the unconsolidated weathered layer derived from in situ decomposition of bedrock, which is commonly known as regolith, saprolite or alterite, which may have a thickness of a few tens of meters, (Mc Farlane 1991; Nahon and Tardy 1992; Thomas 1994; Taylor and Howard 1998), and (2) the fractured rock layer characterized by a dense network of horizontal fractures in the first few meters and a depth-decreasing density of subhorizontal and subvertical

✉ Javier Samper
j.samper@udc.es

1 Universidade da Coruña, Centro de Investigaciones Científicas Avanzadas (CICA), ETS Ingenieros de Caminos, Canales y Puertos, Universidade da Coruña, A Coruña, Spain

2 Universidade de Santiago de Compostela, Escuela Politécnica Superior de Ingeniería, Lugo, Spain

3 Universidade da Coruña, Centro de Investigaciones Científicas Avanzadas (CICA), Facultad de Ciencias, Universidade da Coruña, A Coruña, Spain

fractures (Houston and Lewis 1988; Howard et al. 1992; Cho et al. 2003; Maréchal et al. 2004, 2006; Wyns et al. 2004; Dewandel et al. 2006, 2012). The underlying unfractured and fresh rock is only locally permeable in fracture zones. These conductive fracture zones are much less dense than in the fractured rock layer and their hydrodynamic properties are highly variable (Pickens et al. 1987; Walker et al. 2001; Cho et al. 2003).

The development of a weathering profile requires significant rainfall to ensure mineral hydrolysis and high mean temperatures to favor the kinetics of weathering (Acworth 1987; Wyns et al. 2003; Oliva et al. 2003). Its development requires long periods under stable tectonic conditions; thus, relatively flat topographic areas are required to avoid erosion of weathering products and to favor water infiltration (Dewandel et al. 2006). Deep layers of weathered crystalline rock are common features of landscapes across equatorial Africa, South America and Asia. In Europe, stable tectonic conditions of Carboniferous, infra Permian and infra Triassic in the Primary era, the Early Cretaceous and the early and middle Eocene lasted enough for the formation of thick (20–30 m) weathering profiles (Wyns et al. 2003). They usually have a high porosity and a low permeability and, when saturated, constitute most of the storage capacity of the aquifer. The weathered layer, however, cannot develop in regions of sharp topography where the erosion rate is higher than the rate of weathering (Dewandel et al. 2006). The weathered layer is thin and bedrock outcrops occur due to stripping. A sharp topography also entails a low ratio of annual recharge to runoff component, which, together with a small thickness of the regolith layer, results in a reduction of the water resources buffering and the discharge as highly variable flowrate streams (Taylor and Howard 2000).

Groundwater flow in hard rocks is controlled by the connectivity of the fracture network which depends on the distribution of fracture lengths, orientations and density (Bour and Davy 1998). Fracturing may be caused by cooling stress in the magma and subsequent tectonic activity (Houston and Lewis 1988), lithostatic decompression processes (Davis and Turk 1964; Acworth 1987; Wrigth 1992) and from the weathering process itself (Lachassagne et al. 2001; Cho et al. 2003; Wyns et al. 2004). The presence of horizontal and sub-vertical fracture sets ensures a good connectivity between fractures and an overall anisotropy of the hydraulic conductivity. The fracture hydraulic connectivity decreases with depth and the limited extension of the deeper flowing fractures can lead to a lateral compartmentalization of the aquifer when the groundwater level decreases significantly (Guihéneuf et al. 2014). Rushton and Weller (1985) and Maréchal et al. (2004) estimated an anisotropy ratio near 10 ($K_{horiz} > K_{vert}$).

The proposed conceptualizations of groundwater flow in hard rocks include (Selroos et al. 2002): double porosity models (Barenblatt et al. 1960), discrete fracture models (Lee and Farmer 1993; Long et al. 1982; Dong et al. 2019), parallel plate models (Bear 1993; Lee and Farmer 1993) and equivalent porous media models (Lubczynski and Gurwin 2005; Courtois et al.

2010; Dewandel et al. 2006, 2012). In an equivalent porous media model, the unconsolidated weathering layer is represented by a porous medium. The continuum approach to the fractured rock layer is much more complex due to the heterogeneity, discontinuity and anisotropy of the fracture network. Data from wells next to each other may show differences of several orders of magnitude in the hydraulic conductivity of the fractured layer (Krásný 1997; Dewandel et al. 2006). The simplification of this layer to an equivalent porous media requires assuming relatively well-connected fractures and upscaling hydraulic parameters to regional scale. The fresh basement can be disregarded for groundwater resources management.

Water supply in the scattered rural areas of the Atlantic regions of Europe such as Galicia (Spain) relies on groundwater catchments and wells. The construction of large centralized infrastructures in these areas requires large investments and maintenance costs. Groundwater supply in rural communities is a paramount challenge for the implementation of the European water protection and management regulations (Directive 2000/60/EC) and the quality of water for human consumption (Directive 98/83/EC).

Oia is a rural coastal area of Galicia (Spain) located in a granitic mountain range. Groundwater is used for water supply by private spring catchments at the summit of the mountains, domestic wells and municipal wells. Several alternatives were explored to overcome the water shortages and address the future demand of a planned residential and hotel complex in the Cistercian Royal Monastery of Santa María de Oia. There are no surface-water sources with significant flowrates. The technical and economic feasibility of connecting this area to centralized infrastructures in the neighbor areas is severely limited by the distance to highly populated areas (Eyser 2012a).

The evaluation of the feasibility and sustainability of the future municipal groundwater supply system of Oia has been addressed with a study of the hydrogeology and groundwater management. The study included: (1) the integration of available geological and hydrogeological data into a hydrogeological conceptual model of the study area; (2) the quantification of groundwater recharge with a hydrological water balance model; and (3) the evaluation of several pumping scenarios with a groundwater flow numerical model. The report starts with a description of the study area. Then, the geology and the hydrogeology of the area are presented, after which the groundwater use and the groundwater resources evaluation with a hydrological water balance model are described afterwards. Then, the conceptual and numerical flow models are presented, and finally, the evaluation of several scenarios of expansion of the municipal groundwater supply system is presented. The report ends with the main conclusions.

Study area

The study area is located in Oia on the north Atlantic coast of Spain near the border with Portugal, between the Vigo

Bay and the mouth of the Miño River (Fig. 1). This region covers a narrow straight coastal strip of N–S direction and a mountain range parallel to the coastline. That coastal mountain range functioned as an orographic barrier, providing suitable conditions for fluvio-nival and periglacial slope processes when the sea level was lower than today, in the middle and late Weichselian (Blanco-Chao et al. 2003, 2007). The study area covers a surface of 84 km². It limits to the west with the Atlantic Ocean and to the east with the water divide along the mountain range (Fig. 1). The area presents steep slopes with elevations ranging from sea level to about 590 m above sea level (asl) at ~2 km from the shore. O Vilar and Lavandeira creeks are the most important water channels of the drainage network, and run nearly perpendicular to the shoreline.

The climate in the study area is wet oceanic with relatively abundant rainfall. According to the Köppen classification, the climate is type Csb with mild temperatures and dry and warm summers (Kottek et al. 2006; Peel et al. 2007). Most of the rainfall occurs from October to May. The mean annual temperature and precipitation in the period 2004–2017 are equal to 13.1 °C and 1,149 mm respectively.

Oia municipality is a rural area with scattered low-density population. Land use is strongly linked to the topography. Fractured granites outcrop in areas with steep slopes which are covered with pine and eucalyptus forests. Most of the population is settled in the intermediate zone, which presents moderate slopes. Natural pastures and cultivated areas cover most of the lowest zones where the slopes are nearly flat.
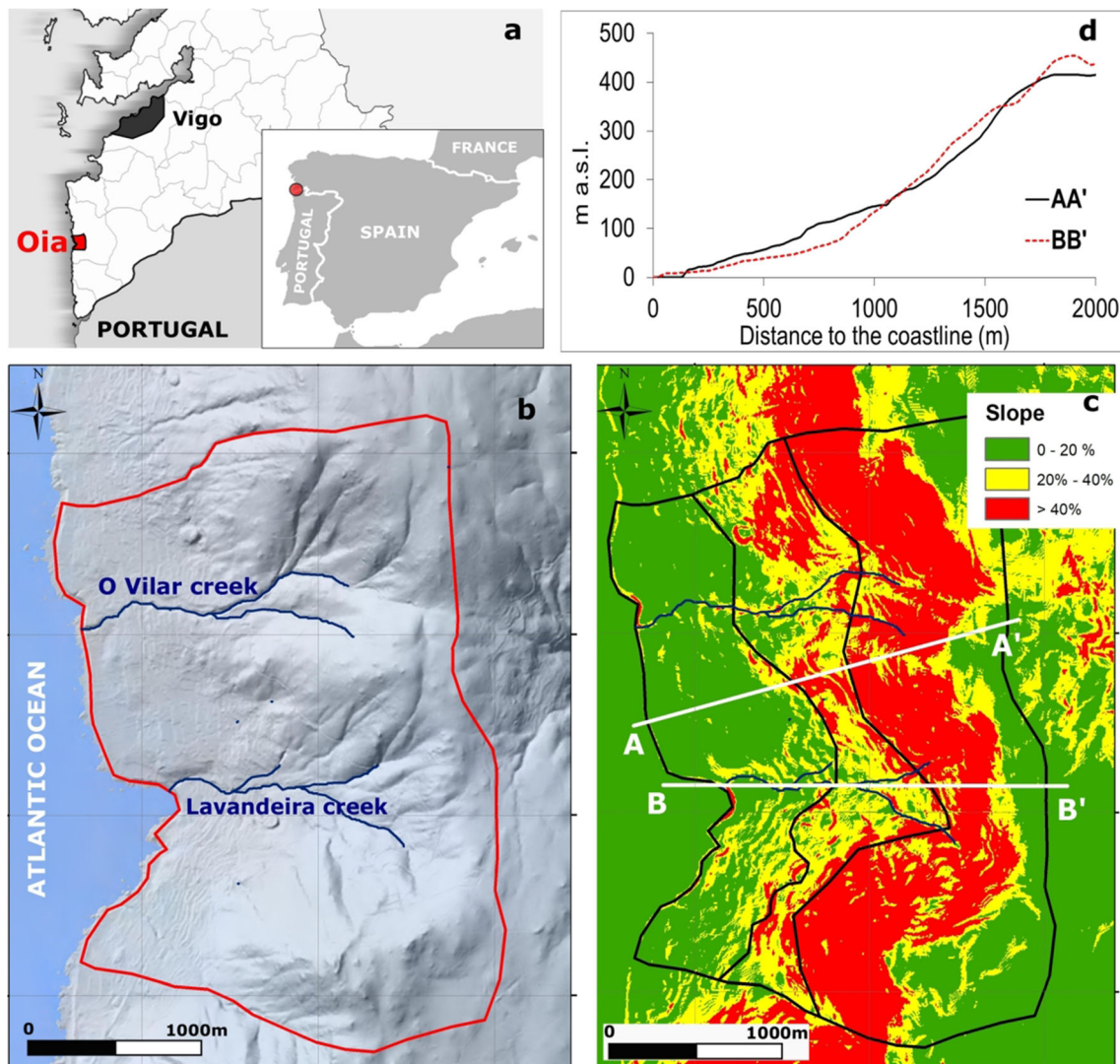

Fig. 1 Location, relief and slope map of the study area: **a** Location map of Oia in Galicia (Spain); **b** Relief map in which the study area is bounded by the red line and the location of O Vilar and Lavandeira creeks is also shown (blue lines); **c** Slope map in which the three homogenous zones in which the domain is divided in the hydrometeorological model are distinguished (black lines) and **d** Topographic cross sections perpendicular to the coast which location is shown in the slope map

Geology

The study area is occupied by two-mica granites formed in the Hercynian orogenesis. These only leave some small enclaves of metasedimentary rocks, which show a high degree of assimilation with the granites and belong to the graywacke schists of the lowest levels of the Ordes Complex (Pliego and Corretge 1978; Pliego et al. 1978; Abril and Corretge 1978a, b). The highest area is formed by less weathered granitic rocks (Fig. 2). The summits of the mountain range are rounded and form a flat area with a weathered granite layer. A few faults of limited extent have been mapped in the study area which are located near O Vilar Creek and run parallel to the coastline.

The metamorphic rocks together with weak terrigenous deposits and alteration soils form a narrow terrace along the coastline, which is characterized by the absence of beaches and the outcrop of granites. The terrace progressively loses height towards the north. The terrace consists of 5–6-m-thick deposits of brownish silts over which a level of thick boulders (up to 20–25 cm in diameter) is superimposed. A boulder beach covers the rearmost 20–75-m-wide shore platform (Pérez-Alberti and Trenhaile 2014). Posthercinic colluvial deposits and slope debris are found downhill, and are formed by sands, silts and granite ridges, coming from the granite degradation, with a chaotic structure and generally with a low degree of compaction.

An electric resistivity tomography (ERT) campaign was performed at O Vilar Creek near wells 1 and 2. The two-dimensional (2D) resistivity tomography was obtained by using the ABEM Lund Imaging system. A multielectrode dipole-dipole configuration was used to collect the resistivity data along a profile with a total of 40 electrodes with 5 m of electrode spacing and a spread length of 200 m (see Fig. 3 for location of the ERT line). The apparent resistivity data were inverted with the RES2DINV software (GeoTomo software) to generate a 2D image of the modelled resistivity along the profile. Topography effects were removed during the interpretation of the resistivity field by using the method of Lu et al. (2015) to avoid misleading ERT anomalies (Fox et al. 1980). The topography along the profile was obtained from LIDAR data. The resistivity model obtained from the inversion of the apparent resistivity data shows a large interval of resistivities, which range from 100 to 30,000 Ω-m. Resistivities show large horizontal and vertical heterogeneities (Fig. 3). The resistivity field allows the identification of the contact of the slope debris and the fractured granite as well as the interface of the colluvial deposits and fractured granite. The approximate thickness of the slope debris in this area is equal to 15 m. A remarkable heterogeneity in resistivities is detected between wells 1 and 2.

Hydrogeology

Piezometric data

Hydraulic head and water quality data were collected at domestic dug wells and boreholes, municipal wells 1–6 (Fig. 4), a regional monitoring piezometer (RMP) of the Galicia-Costa hydrological district, spring catchments and public groundwater fountains. Most of the springs are located in the highest zone along the contact between the flat mountain summit, in which rocks are covered by a significant layer of regolith, and the steepest slope hillside where fractured rocks outcrop. A few springs are scattered in the intermediate and the lowest zones of the study area (Fig. 4). Available hydraulic head data
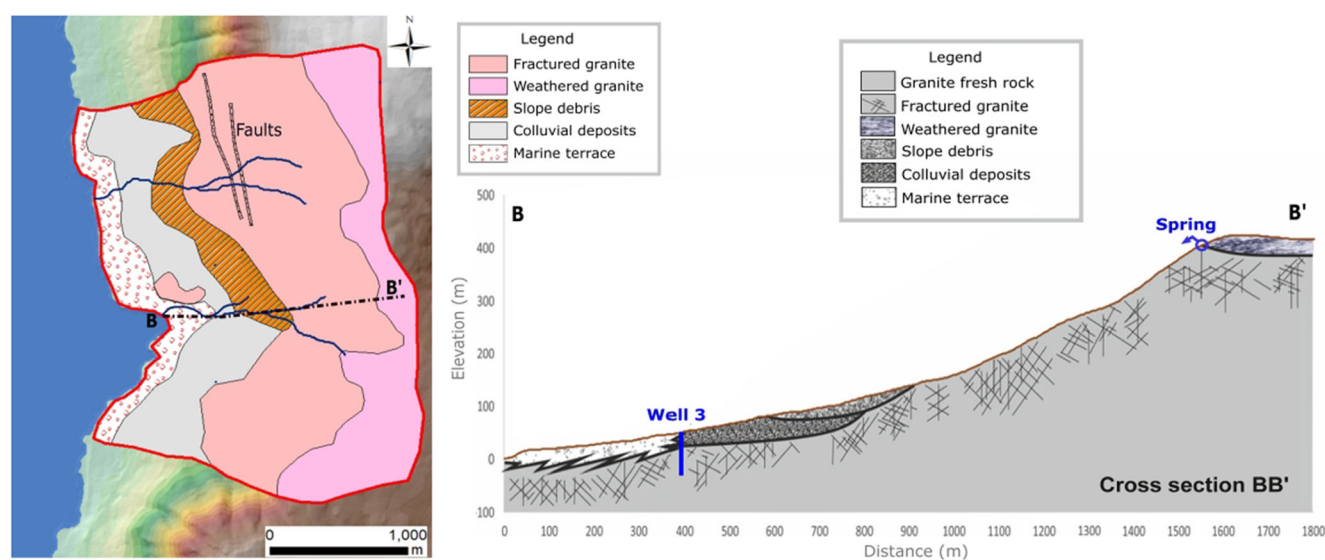

Fig. 2 Geological map of the study area and vertical cross-section along Lavandeira Creek (BB′) illustrating the hydrogeological conceptual model. The profile extends from the coast to the summit of the mountain range and its location is shown in the geological map
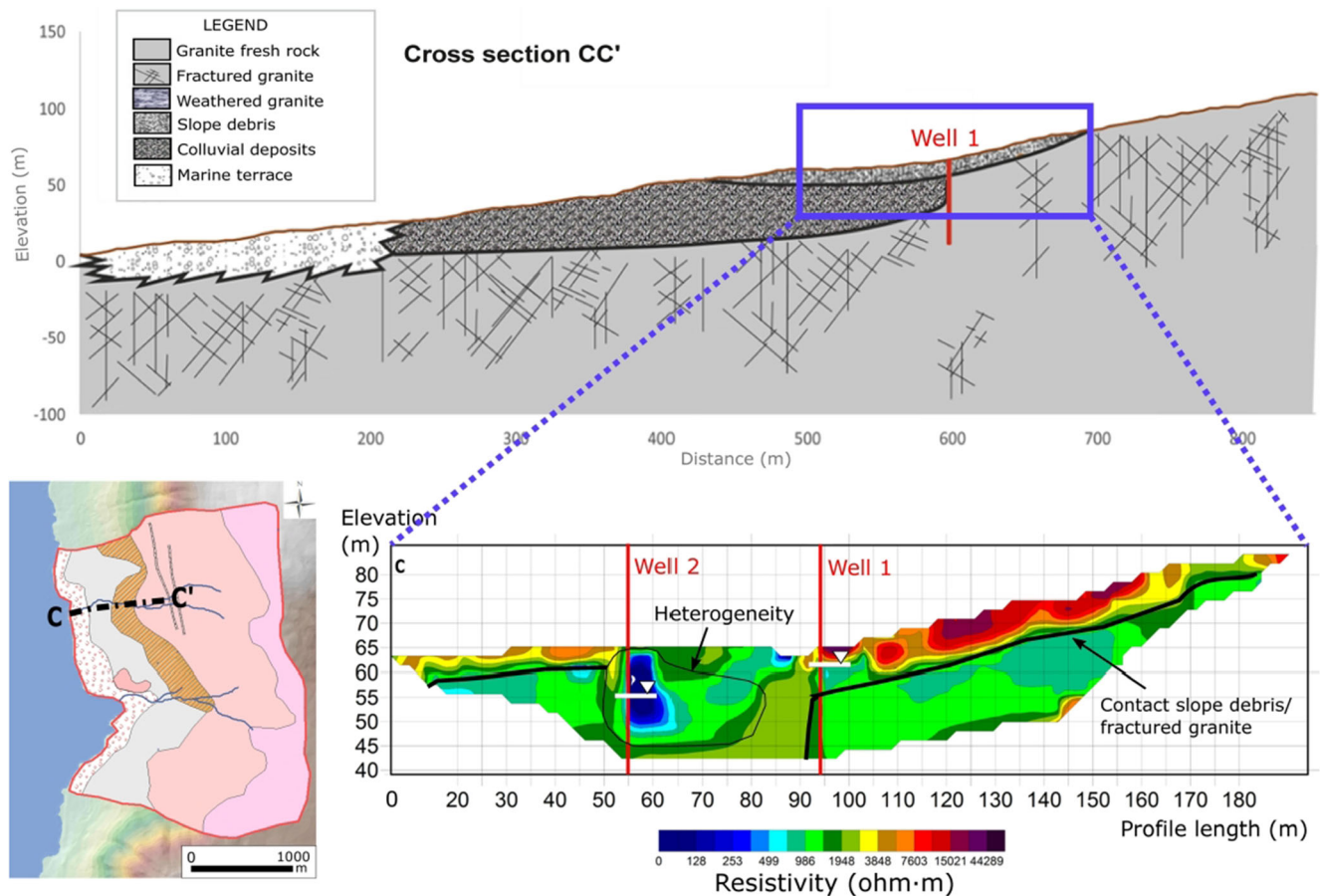
Fig. 3 Vertical cross-section along O Vilar Creek illustrating the hydrogeological conceptual model (top), with location shown in the geological map, and vertical profile of the resistivities obtained from the inversion of the 2D tomographic data (bottom), including the location of the wells (red lines) and the measured groundwater levels in the wells (white symbols)

show that the water table is generally shallow, with a depth less than 10 m in most of the study area. Head data recorded at the RPM from 2011 to 2014 show that: (1) the water table rises in response to rainfall events, and (2) the seasonal oscillations of the hydraulic heads are smaller than 1.5 m (Fig. 5).

A contour map of hydraulic heads in the intermediate and the lowest zones of the study area is shown in Fig. 4. The contour lines of hydraulic heads are nearly parallel to the topographic contour lines, showing that the groundwater flows from the top of the mountains towards the sea and towards Lavandeira and O Vilar creeks. The average hydraulic head gradient is ~0.1 m/m.
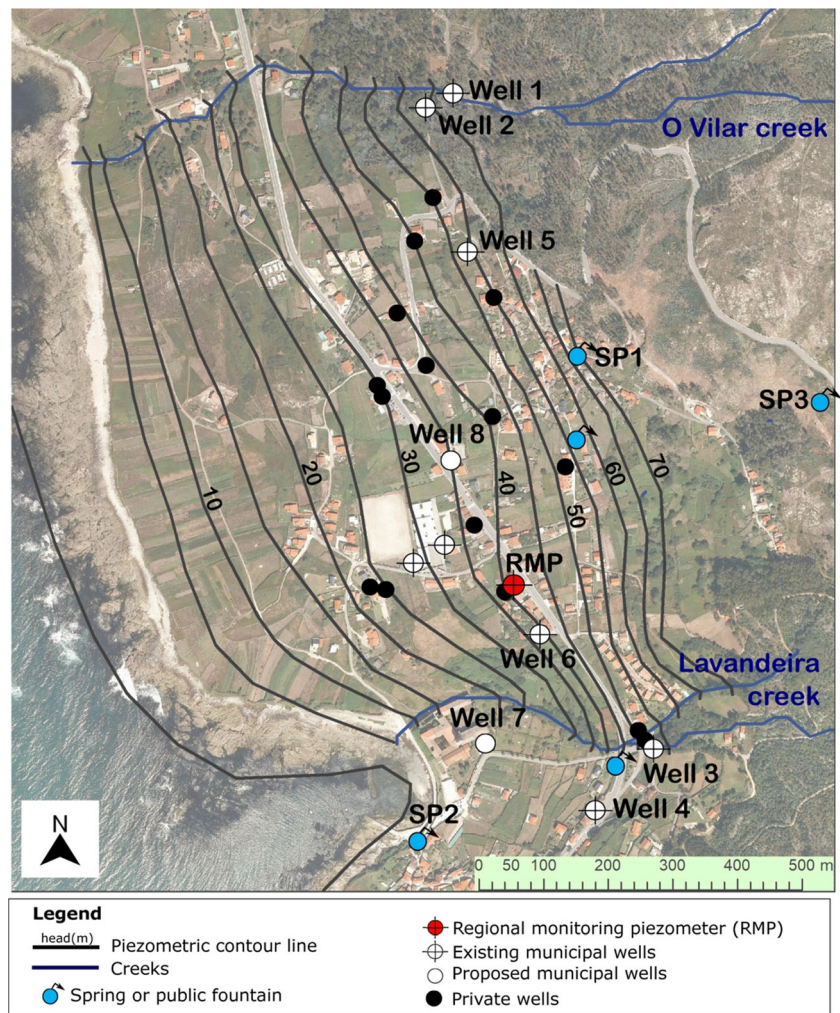
Pumping tests

Several exploratory drillings were performed by the Oia municipality in the study area. About half of them failed or provided very low yields. Several pumping tests were performed in the most productive wells located near the creeks with different pumping rates and durations (Fig. 4). Well 1 is 57 m deep and is located near O Vilar Creek. It

was drilled on slope debris which overly the fractured granite. A well yield of about 1.5 L/s was recorded with a drawdown of 1 m when the depth to the water table was <2 m. The alluvial deposits of the creek provide a high water yield. Drawdowns of ~40 m were recorded for a pumping rate of 2.5 L/s when the depth to the water table exceeded 3 m. The estimated transmissivity (T) of the slope debris and fractured granite ranges from 0.7 to 1 m^2/day. Well 2 is 50 m away from O Vilar Creek. The drilling airlift yield of well 2 was significantly smaller than that of well 1, thus showing the heterogeneity of the slope debris.

Wells 3 and 4 were the most productive drillings near Lavandeira Creek. They were drilled in colluvial deposits near the contact with the marine terrace. Well 3 is 65 m deep. The estimated well yield was about 1.6 L/s with a drawdown equal to 37 m. Alluvial deposits of the creek were found over the colluvial deposits in well 3, showing transmissivities about 20 m^2/day. These deposits have a very limited areal extent and therefore can be disregarded. The estimated T of the underlying colluvial deposits and

Fig. 4 Piezometric map in a strip of the study area by the coast between O Vilar and Lavandeira creeks. Piezometric head of contour lines is expressed in meters (m). The locations of the piezometer of the regional monitoring network (RMP), the existing and proposed municipal wells, the inventoried private wells and the springs and fountains in the area are indicated with different symbols. Water samples for physico-chemical and microbiological analyses were taken in wells 1–4 and springs SP1, SP2 and SP3. Notice that the location of the spring SP3 is related to the sampling point in a private small supply network but sampled water comes from several springs located near the summit of the mountains

fractured granite ranges from 0.6 to 1.4 m²/day. Well 4 is 60 m deep and about 100 m away from Lavandeira Creek (Fig. 2). The estimated yield of well 4 was about 1 L/s for a drawdown of 32 m.

The results of the pumping tests show that the maximum pumping rate in well 1 near O Vilar Creek is equal to 200 m³/day, except during the dry season (July–September) when the maximum rate is 40 m³/day. The pumping rates in wells 3 and
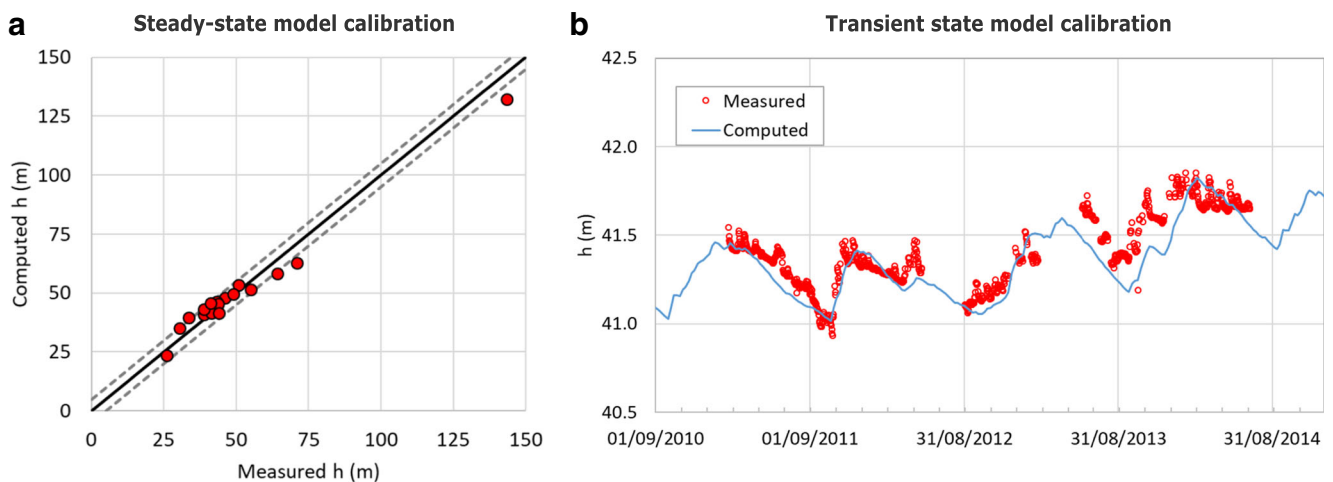

Fig. 5 **a** Scattergram of the computed and the measured steady-state heads in the observation wells in which dashed lines represent an error of ±5 m. **b** Time evolution of the computed transient head (line) and measured (symbols) at the regional monitoring piezometer (RMP)

4 near Lavandeira Creek are estimated to be equal to 150 and 90 m^3/day, respectively.

Lavandeira and O Vilar creeks

Weekly gauging campaigns were carried out in the Lavandeira and O Vilar creeks from May to September of 2017. These data were supplemented with qualitative observations during several field campaigns. Lavandeira Creek maintains a permanent flow all year long, especially at its lowest stretch. Measured flow rates during the dry season range from 0.1–4.5 L/s. This creek has springs throughout its course. Water springing up on its banks was observed in a stretch ~100 m downstream from well 3 after several days without rainfall. The water table near Lavandeira Creek is shallow (~3 m deep).

Available data show that Lavandeira Creek is a discharge zone, at least in the lower stretches when the water table is high. On the other hand, the creek may act as a recharging zone when the water table drops, as attested by the stabilized drawdowns recorded in pumping tests performed in wells 3 and 4 near the creek.

Field data show that O Vilar Creek is a discharge zone in some stretches in winter when the water table is high. On the other hand, the creek was dry during 90% of the weekly gauging campaigns performed during the dry season. According to communication with local residents, the current morphology of O Vilar Creek reflects the consequences of the floods that occurred after a big fire in the summer of 2013. The bed of the creek was filled with large boulders and pebbles dragged during floods. There might probably be a subsurface flow that runs below the bed of boulders even when the channel is dry on the surface. The available streamflow data from O Vilar Creek clearly underestimates the actual discharge because: (1) the morphology of the creek does not allow an accurate gauging of the creek; and (2) most of the discharge data were collected during the dry season when the creek was dry.

Groundwater chemistry

Available groundwater chemical and bacteriological data include: (1) 20 water samples from the regional monitoring piezometer (RPM) from 2012 to 2015; (2) 3 water samples from 2012 in springs SP1 and SP2 and in a tank of a private water supply system, where water from several springs located at the highest area is stored; and (3) 4 samples collected in 2017 from wells 1–4. Figure 4 shows the location of the sampling points. The following parameters were measured: temperature, pH, Eh, dissolved oxygen, electrical conductivity (EC), concentrations of major cations and anions, concentrations of Fe, Al, Mn and heavy metals (As, Cd, Cu, Zn, Cr, Sn, Sr, Hg, Ni, Pb and Se) and microbiological presence.

Table 1 shows the measured values of pH, EC, and the concentrations of the main cations and anions. Groundwater is slightly acidic, with a pH range between 5.46 and 6.46. The electrical conductivity is low and ranges from 78 to 204 µs/cm. The most abundant hydrochemical facies is sodium/chloride. The cation composition is similar in all samples while the differences occur in bicarbonate and sulphate.

The measured concentrations of the cations and anions are below the parametric values for drinking water (RD 140/2003; EC 2010). No significant nitrate contamination is observed. Groundwaters in the study area show a slight bacteriological contamination. This contamination is avoided by the chlorination of the municipal supply system.

Groundwater uses and resources

Groundwater uses

The current groundwater municipal use ranges from 25 to 30 m^3/day. Private groundwater use from spring catchments and wells is estimated to be equal to 118 m^3/day. Private water consumption increases in the summer due to seasonal population, garden irrigation and use of swimming pools. Assuming a seasonal peak consumption factor of 1.4, the peak groundwater consumption is ~200 m^3/day.

The population of Oia has remained nearly constant during the last 10 years. No significant increase in water demand is foreseen in the study area, except for the development of a tourist center in the former Cistercian Royal Monastery of *Santa María de Oia*. According to the "Technical instructions for hydraulic works in Galicia" (Aguas de Galicia 2011), the water demand of the touristic complex will be ~500 m^3/day; thus, the expected total future demand in the study area is estimated to be ~700 m^3/day.

Hydrological model

Groundwater recharge comes from the infiltration of precipitation throughout the study area. Its magnitude varies spatially and temporally, with the spatial variability depending mainly on the terrain slope, geology and land use.

A hydrological water balance model was performed to evaluate the groundwater resources in the study area. The hydrological model was carried out with VISUAL-BALAN, a semidistributed hydrological code which solves daily the water balance in the soil, the unsaturated zone and the aquifer (Samper et al. 1999, 2015a, b; Stigter et al. 2014; Pisani et al. 2019).

Table 1 Chemical data from groundwater samples taken in the study area. The location of the sampling points is shown in Fig. 4

Parameter	RMP[a]	Well 1	Well 2	Well 3	Well 4	Spring 1 (SP1)	Spring 2 (SP2)	Spring 3 (SP3)
pH at 20 °C	6.18	5.46	5.81	6.37	6.46	5.76	6.09	6.25
EC at 20 °C (µS/cm)	142	78	87	108	204	143	184	95
Chloride (mg/L)	27.6	19.7	19.9	20.2	29.3	33.7	33.8	21.3
Sulphate (mg/L)	19.5	3.2	4.7	4.3	10.0	4.4	10.9	3.5
Bicarbonate (mg/L)	13.8	17.1	12.2	20.3	43.6	9.0	6.3	7.5
Nitrate (mg/L)	4.9	<0.4	0.6	1.2	6.8	2.6	15.1	2.8
Sodium (mg/L)	15.9	13.0	13.0	15.0	27.0	19.1	19.7	11.9
Calcium (mg/L)	3.87	<1.30	1.47	3.00	9.01	1.30	4.80	0.92
Magnesium (mg/L)	1.83	1.43	1.63	2.11	3.70	2.10	2.60	1.60
Potasium (mg/L)	4.51	<0.50	0.59	0.55	3.80	1.06	5.28	1.09
Predominant lithologies	Colluvial deposits/-fractured granite	Slope debris, colluvial deposits and fractured granite	Slope debris, colluvial deposits and fractured granite	Colluvial deposits & fractured granite near marine deposits	Marine deposits and fractured granite	Slope debris/-fractured granite	Marine deposit-s/ fractured granite	Weathered granite

[a] Mean value of 20 water samples

The watershed was divided into three homogeneous zones, which are strip-shaped and oriented parallel to the shoreline (Fig. 1). Steep slopes are prone to high rates of surface runoff and interflow and small recharge rates (Gurtz et al. 2003; Wu and Xu 2005; Espinha Marques et al. 2010, 2013; Samper et al. 2015a). The steepest slope in the highest part has the lowest recharge, whereas the recharge is largest in the marine terrace at the sea level.

The parameters of VISUAL-BALAN are constant in each homogeneous zone (Samper et al. 2007). The meteorological data were measured at the Castro-Vicaludo meteorological station located at an elevation of 473 m asl. The model parameters were calibrated by fitting the computed hydraulic heads to the measured piezometric data from 2011 to 2014 in the regional monitoring piezometer (RMP). Similar to Espinha Marques et al. (2010), the results of the hydrological water balance model are highly sensitive to soil thickness, whereas the computed groundwater recharge is most sensitive to the interflow and percolation recession coefficients. The mean annual groundwater recharge is 108 mm/year, ranging from 73 mm/year in the steepest zone to 135 mm/year in the lowest zone. The average groundwater resources in the study zone range from 1,330 m³/day in dry years to 2,467 m³/day in wet years. Average groundwater resources in the study area are larger than the estimated future groundwater demand (~700 m³/day).

Conceptual hydrogeological model

A regolith layer of significant thickness is present in the nearly flat summit of the mountains where erosion was less intense and allowed the formation of the regolith. The granitic rock is significantly fractured near the surface and it is fresh in depth. Downhill of the mountain, the fractured granite is covered by the detrital formations such as slope debris, colluvial deposits and marine terrace. Figure 2 shows the hydrogeological profile between the coast and the highest area of the mountain range along Lavandeira Creek.

The average thicknesses of the regolith and the fractured granites in the study area were taken equal to 25 and 60 m, respectively, based on the values reported by Wyns et al. (2003). The thickness of the detrital formations was estimated from geophysical surveys (Fig. 3) and the calibration of the numerical groundwater flow model.

The gradient of the water table is high because the hydraulic conductivities of the geological formations of the study area are generally low. Most of the groundwater flows through the regolith and the detrital formations, which have a hydraulic conductivity significantly larger than that of the fractured granite. Groundwater flows through the fractured granite only in places where it outcrops. Otherwise, groundwater flows through the regolith and the detrital formations. The faults in the granitic rocks do not play a relevant role in groundwater

flow according to the available field data. Piezometric head data show that groundwater flows from the highest parts of the mountain range towards the coastline and towards Lavandeira and O Vilar creeks. Both creeks are discharge zones when the water table is shallow; on the other hand, the creeks become losing creeks when the water table drops in the summer or due to groundwater pumping. Water accumulates in the regolith and flows through this layer towards the hillside, where fractured granite outcrops (Fig. 2). Although most springs are located along the contact of the regolith layer with the fractured granite in the hillside, some springs are also found at lower elevations in detrital formations near the outcrops of granitic rocks.

The fractured granite is assumed to behave as an equivalent porous medium. Groundwater flow is assumed to be 2D and nearly parallel to the water table. Vertical groundwater flow is disregarded. Most of the pumping and observation wells are not affected by changes in water density; therefore, the spatial variability of water density near the coast is disregarded.

Groundwater flow numerical model

A 2D groundwater flow numerical model was performed to test the conceptual model with field data and evaluate the feasibility of expanding the municipal water supply system to provide the future water demands. The numerical model was calibrated by using the available piezometric data. Afterwards, it was used to simulate pumping scenarios and compute groundwater drawdowns and evaluate the potential for seawater intrusion.

The model domain was discretized with a finite element mesh of 2,426 nodes and 4,764 triangular elements (Fig. 6). The mesh was refined along the creeks and near the pumping wells. The estimates of groundwater recharge rates in the three homogeneous zones considered in the hydrological water balance model were used as inputs to the groundwater flow model. The numerical model accounts for groundwater discharge along the coast, along O Vilar and Lavandeira creeks, at the springs located along the regolith/fractured granite contact at the summit of the mountains and at the springs in detrital formations near rock outcrops. The hydraulic head (h) is prescribed and equal to 0 along the coast. Lavandeira and O Vilar creeks and the springs are simulated with a Cauchy boundary condition according to which the nodal flux, Q (m³/day), is equal to $\alpha \cdot (h_{ext} - h)$, where α is a leakage coefficient (m²/day), h is the hydraulic head and h_{ext} is an external head which is taken equal to ground surface elevation. The leakage coefficients were taken equal to 100 m²/day to ensure that the computed hydraulic heads at the boundaries are equal to the h_{ext}.

The rest of the model boundaries are water divides and are assumed impervious. The model accounts for 10 hydraulic conductivity and specific yield zones which were defined
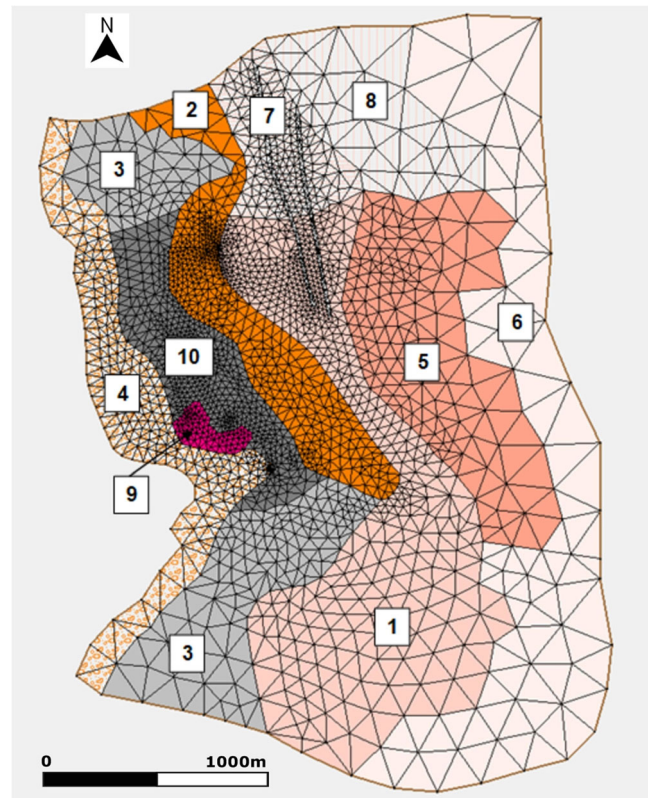

Fig. 6 Finite element mesh and hydraulic conductivity zones of the 2D groundwater flow numerical model. Zones 1, 5, 7, 8 and 9 are related to fractured granite, zone 6 to weathered granite, zone 2 to slope debris, zones 3 and 10 to colluvial deposits, and zone 4 to the marine terrace

based on the hydrogeological conceptual model (Fig. 6). The saturated thickness of the fractured granite, the regolith and the slope debris were estimated from geophysical surveys and published data. They are equal to 60, 25 and 15 m, respectively (see Table 2). The thickness of the colluvial deposits and the marine terrace was derived from groundwater flow model calibration and was taken equal to 20 m (Table 2).

Table 2 Calibrated transmissivities (T), specific yield (S_y) and thickness (b) of the parameter zones considered in the groundwater flow model. The geometry of the zones is shown in Fig. 6

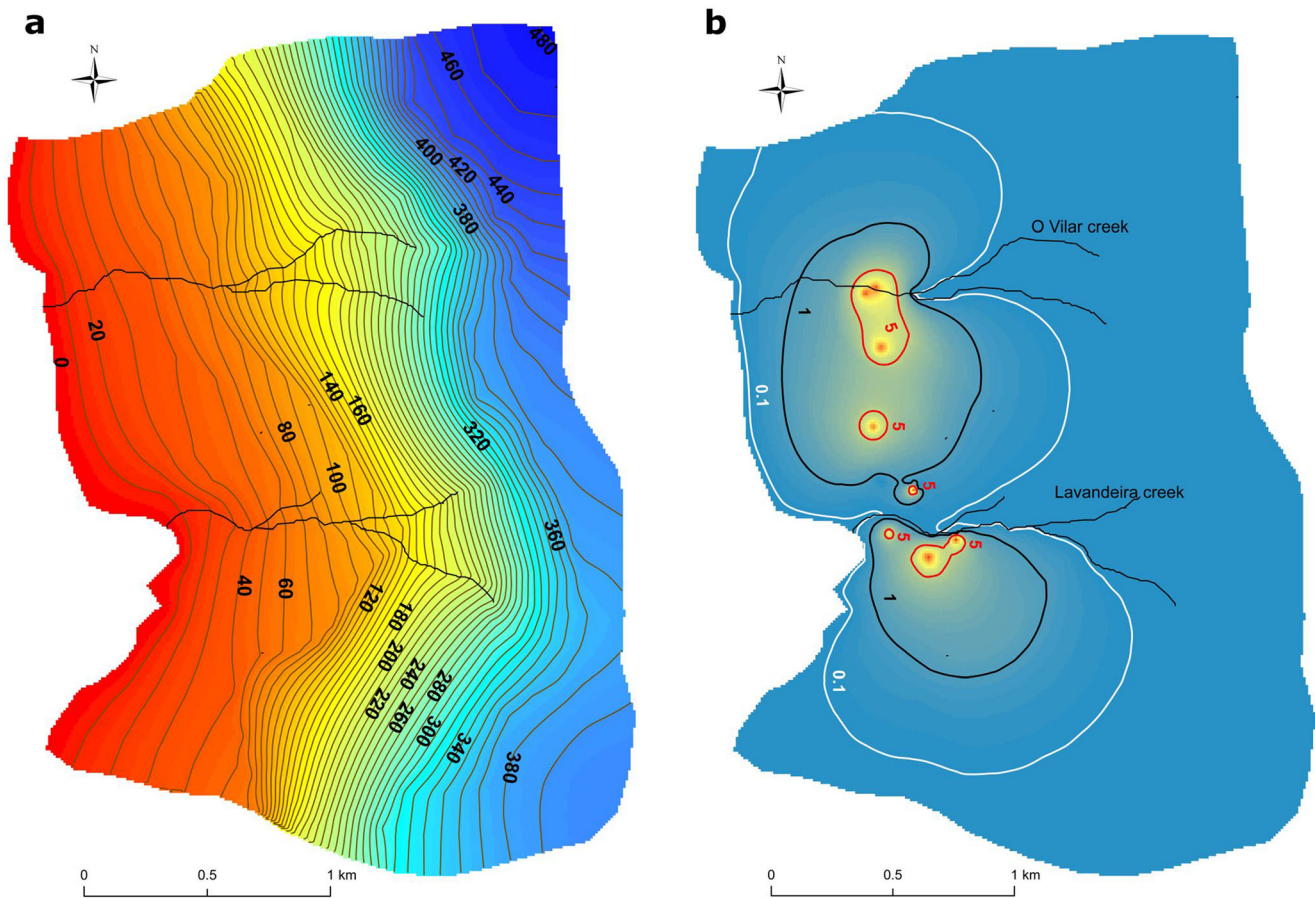| Geological formation	Zone number	T (m²/day)	S_y (−)	b (m)
Fractured granite	1	0.35	0.009	60
	5	0.25		
	7	0.55		
	8	0.25		
	9	0.9		
Weathered granite	6	1.2	0.125	25
Slope debris	2	1.4	0.112	15
Colluvial deposits	3	4.5	0.150	20
	10	5.1		
Marine terrace	4	4	0.150	20

Fig. 7 Contour lines of the **a** computed steady-state hydraulic heads (lines every 10 m) and **b** computed drawdown (s) during the dry season for the maximum pumping rates in wells 1–8. White, black and red lines correspond to $s = 0.1$, 1 and 5 m, respectively. The maximum drawdowns in O Vilar and Lavandeira creeks are equal to 15.9 and 15.4 m, respectively

The groundwater flow numerical model was performed with CORE^{2D} (Molinero et al. 2004; Samper et al. 2009, 2012; Lu et al. 2011; Águila et al. 2019; Naves et al. 2019). The model was calibrated in two stages. In the first stage, the transmissivities were calibrated under steady-state conditions by using prior information on transmissivities from pumping tests and ensuring that the computed hydraulic heads match the measured heads. The absolute value of the calibration head errors is smaller than 5 m (Fig. 5). The calculated Nash index is almost equal to 1. Figure 7 shows the contour map of the computed water table.

Table 3 presents the recharge and discharge components of the steady-state groundwater balance in the model domain. Groundwater recharge in the model domain is equal to 1,978 m^3/day. Most of the groundwater discharges to the sea (72%), while 12% discharges in springs and 16% along the creeks. The computed discharge in Lavandeira Creek (174 m^3/day) is within the range of the gauged values. The computed discharge along O Vilar Creek is larger than the measured flow rates which underestimate the actual discharge.

In the second calibration stage, the storage coefficients were calibrated under transient conditions by using the

piezometric data recorded at the Oia RMP piezometer from 2011 to 2014. The computed hydraulic heads match the measured heads (Fig. 5). Model results validate the recharge rates estimated with the hydrological water balance model.

Table 3 Components of the steady-state groundwater balance in the domain of the groundwater flow model of the study area

Balance component	Q (m^3/day)	Percentage
Recharge	1,978	100%
Highest zone	724	37%
Intermediate zone	852	43%
Lowest zone	402	20%
Discharge	1,913	100%
Coast line	1,383	72%
Springs	229	12%
O Vilar Creek	127	7%
Lavandeira Creek	174	9%
Water balance error		3.2%

Table 4 Comparison of calibrated values of the hydraulic conductivity (K) in the groundwater flow numerical model of Oia with estimated K from the interpretation of the hydraulic tests and estimated K values for other granitic formations in the literature. NA not available

Geological formation	Calibrated K (m/day)	K (m/day) derived from tests	Estimated K (m/day) in other granitic areas	
Fractured granite	0.004–0.015	NA	0.4–0.7	Taylor and Howard (2000)
			0.26	Houston and Lewis (1988)
			1.73	Maréchal et al. (2004, 2006)
			4.32	Rushton and Weller (1985)
Weathered granite	0.05	NA	0.008–2.6	Taylor and Howard (2000)
			0.05–3.5	Houston and Lewis (1988)
			0.006–0.86	Compaore et al. (1997)
			0.35–0.5	Rushton and Weller (1985)
			0.06–2.5	Dewandel et al. (2006)
Slope debris	0.09	~0.06		
Colluvial deposits	0.34	~0.05		
Marine terrace	0.20	NA		

Table 2 lists the calibrated transmissivities and specific yields of the parameter zones. The calibrated hydraulic conductivities (K) have been compared to the conductivities derived from the interpretation of the pumping tests and the conductivities reported in the literature for granitic formations (see Table 4). The calibrated conductivities for the fractured granite range from $4 \cdot 10^{-3}$ to $1.5 \cdot 10^{-2}$ m/day. These values are lower than the values compiled from the literature. This discrepancy of the Oia site might be explained by the erosion of the shallowest and most fractured granite, due to the steepness of the hillside and its great exposure to rain and wind, resulting in a less thick and fractured granite. The calibrated conductivity of the regolith (K) is equal to 0.05 m/day. The calibrated K is within the range of published values (Table 4). The calibrated hydraulic conductivity K could be larger than 0.05 m/day if the thickness of the regolith is smaller than 30 m. The calibrated conductivity of the slope debris coincides with the value estimated from the pumping test performed in well 1. On the other hand, the calibrated conductivity of the colluvial deposits is an order of magnitude larger than the conductivity estimated from the pumping test performed in well 3.

Evaluation of several scenarios of expansion of municipal groundwater supply

The water-table drawdowns and seawater intrusion were evaluated for two pumping scenarios with a 2D numerical groundwater flow model. Pumping scenarios include the combination of the existing wells (wells 1–6) and additional wells (wells 8 and 9). Pumping rates vary seasonally. The pumping rate is largest in the summer and smallest in the winter. Figure 8 shows the dimensionless pumping rate function considered in the pumping scenarios. The actual pumping rate is equal to the product of the dimensionless pumping rate function times the maximum pumping rate, Q_{max}. An acceptable scenario is one which produces moderate drawdowns (<20 m), no seawater intrusion and limited drawdowns in existing domestic wells.

The first scenario considers four existing municipal wells with the following maximum pumping rates: 25 m³/day in wells 1 and 2, 250 m³/day in well 3 and 150 m³/day in well 4 (Table 5). Model results show that the pumping rates of wells 1 and 2 should be limited to 6 m³/day in the dry season and 25 m³/day in the rest of the year. Figure 9 shows the computed drawdowns in wells 1–4. The maximum

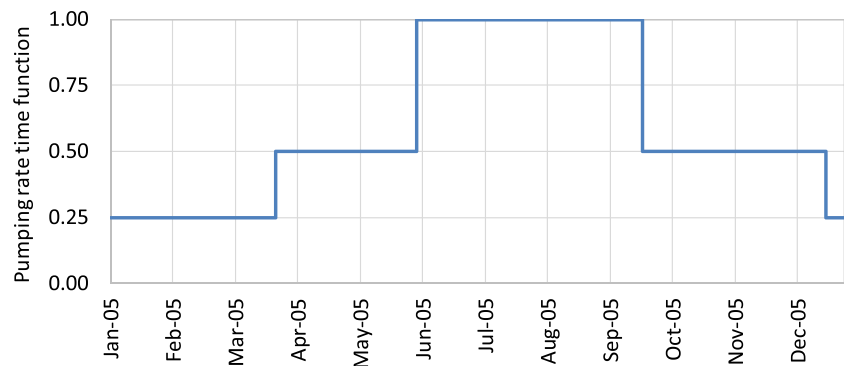**Fig. 8** Dimensionless pumping rate function

Table 5 Maximum and average pumping rates used in the numerical model

Well No.	Q_{max} (m³/day)	Average Q (m³/day)
1	25	15
2	25	15
3	250	148
4	150	89
5	35	21
6	35	21
7	70	41
8	100	59

drawdowns are equal to 14.9 m near O Vilar Creek (wells 1 and 2) and 15.6 m near Lavandeira Creek (wells 3 and 4). The total maximum pumping rate of the current municipal system is 450 m³/day. Therefore, it can be concluded that the future estimated demand (~700 m³/day) cannot be satisfied with the current groundwater supply system and additional pumping wells are required.

Scenario 2 considers wells 1–4 and the following additional four wells: (1) the existing municipal well 5 located south of O Vilar Creek in the intermediate zone of the slope scree; (2) the existing municipal well 6 located north of Lavandeira Creek in the colluvial deposits; (3) a proposed new well in the marine terrace near Lavandeira Creek (well 7); and (4) a proposed new well (well 8) located in the colluvial deposits near wells 5 and 6. The maximum pumping rates of wells 1–4 are similar to those
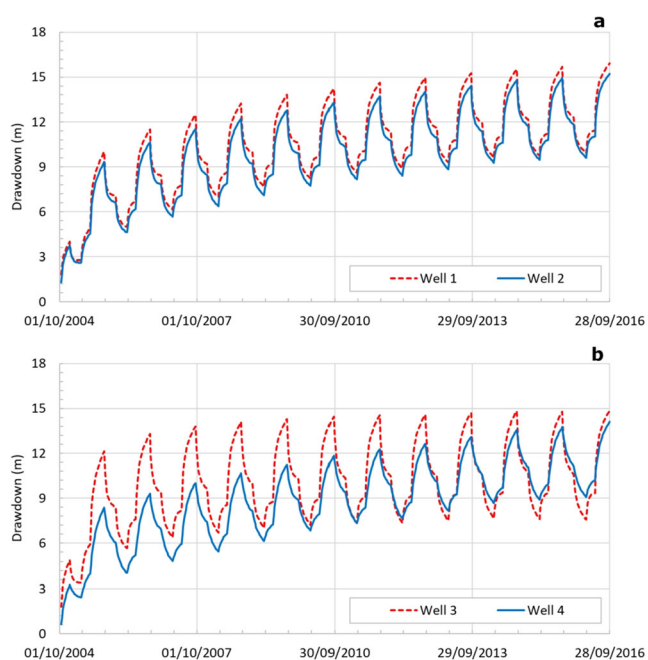
Fig. 9 Time evolution of the computed drawdowns in **a** wells 1 and 2 and **b** in wells 3 and 4

of the first scenario. The maximum pumping rates in wells 5 and 6 are equal to 35 m³/day, while those of wells 7 and 8 are equal to 70 and 100 m³/day, respectively (Table 5).

Figure 7 shows the map of the computed drawdowns at the end of the dry season for scenario 2. The maximum computed drawdowns in wells 5, 6, 7 and 8 are equal to 14.1, 14.2, 7.4 and 13.4 m, respectively. Figure 9 shows the computed drawdowns in wells 1–4. The total maximum pumping rate in scenario 2 is about 690 m³/day during the dry season, while the average pumping rate is about ~400 m³/day. Model results of scenario 2 show no significant effects on existing wells. The potential impact of pumping wells on seawater intrusion was analyzed by computing the decrease of the discharge rate of fresh groundwater into the sea along the coastal line compared to the natural discharge rate. The total groundwater discharge after 6 years of pumping decreases 7.5%. The maximum decrease is 18% at the mouth of Lavandeira Creek. This small reduction in groundwater discharge is not expected to lead to a significant advance of the saline wedge. It is concluded that no seawater intrusion is expected in scenario 2.

Conclusions

A hydrogeological study of a coastal granitic area having unique geomorphological and hydrogeological features with steep slopes favoring the erosion of the weathered granite, has been presented. The steep slopes and the great exposure of the hills to rain and wind promote the erosion of the weathered and altered granite. The regolith layer is present only at the flat summit of the mountains and is not formed on the hillside where the fractured granite is barely covered. The proposed hydrogeological conceptual model of the study area includes: (1) the regolith, which is present only in the flat summit of the mountains; (2) the fractured granite which lies below the soil in the hillside; (3) the slope debris and the colluvial deposits, which are present in the intermediate and the lowest parts of the hillside; and (4) the marine terrace. Water accumulates in the regolith and flows through this layer, having a hydraulic conductivity significantly larger than that of fractured granite, towards the hillside. Most of the springs are for domestic use and are found at the contact of the regolith with the fractured rock along the hillside (Eyser 2012b). Slope debris and colluvial deposits are present in the intermediate and lowest parts of the hill slope. The regolith and the detrital layers exhibit a hydraulic conductivity larger than that of the fractured granite.

Groundwater resources in the study area have been evaluated with a hydrological water balance model. Average aquifer recharge ranges from 73 mm/year in the steepest zones to 135 mm/year in the lowest areas. Thus, average groundwater resources are equal to 2,000 m³/day, which are sufficient to

supply the estimated current groundwater use (200 m^3/day) and the foreseen future needs (700 m^3/day).

The conceptual hydrogeological model has been implemented in a groundwater flow numerical model, which later has been used to evaluate the performance of two pumping scenarios and select the optimum solution to attain sustainable conditions. The results of the numerical groundwater flow model confirm the validity of the proposed conceptual hydrogeological model, which for the most part is consistent with the available geophysical, geological and pumping test data as well as with the conceptual models reported in the literature.

Model predictions show that the needs for domestic and tourist water supply can be safely provided with groundwater pumping wells with admissible drawdowns and no seawater intrusion. Our study illustrates that the combination of a sound conceptual hydrogeological model, a hydrological water balance model and a numerical groundwater flow model provides a robust tool to evaluate the feasibility and sustainability of groundwater supply systems.

The results of our study could be improved by: (1) performing a more detailed piezometric and hydraulic characterization of the study area with additional field tests, especially in the regolith, the fractured granites and the marine terrace; and (2) collecting water samples directly in spring catchments instead of water samples from water tanks.

References

Abril J, Corretge LG (1978a) Geologic map of Spain (MAGNA), scale 1: 50.000, sheet 298: La Guardia. Instituto Geológico y Minero de España (IGME), Madrid

Abril J, Corretge LG (1978b) Geologic map of Spain (MAGNA), scale 1: 50.000, sheet 299: Tomiño. Instituto Geológico y Minero de España (IGME), Madrid

Acworth RI (1987) The development of crystalline basement aquifers in a tropical environment. Q J Eng Geol 20:265–272

Aguas de Galicia (2011) Instruccións Técnicas para Obras Hidráulicas en Galicia, vol 1 [Technical instructions for hydraulic works in Galicia, vol 1]. https://augasdegalicia.xunta.gal/c/document_library/get_file?folderId=216484&name=DLFE-17837.pdf. Accessed 8 March 2021

Águila JF, Samper J, Pisani B (2019) Parametric and numerical analysis of the estimation of groundwater recharge from water-table fluctuations in heterogeneous unconfined aquifers. Hydrogeol J 27:1309–1328. https://doi.org/10.1007/s10040-018-1908-x

Barenblatt GI, Zheltov IP, Kochina IN (1960) Basic concepts in the theory of seepage of homogeneous liquids in fissured rocks. Appl Math Mech 24 (5):852–864

Bear J (1993) Modeling flow and contaminant transport in fractured rocks. In: Bear J, Tsang C, de Marsily G (Eds.), Flow and Contaminant Transport in Fractured Rocks. Academic Press, San Diego, pp 1–36

Blanco-Chao R, Costa Casais M, Martínez Cortizas A, Pérez Alberti A, Trenhaile AS (2003) Evolution and inheritance of a rock coast: western Galicia, northwestern Spain. Earth Surf Process Landf 28: 757–775. https://doi.org/10.1002/esp.496

Blanco-Chao R, Pérez-Alberti A, Trenhaile AS, Costa-Casais M, Valcárcel-Díaz M (2007) Shore platform abrasion in a para-periglacial environment, Galicia, northwestern Spain. Geomorphology 83(1–2):136–151. https://doi.org/10.1016/j.geomorph.2006.06.028

Bour O, Davy P (1998) On the connectivity of three-dimensional fault networks. Water Resour Res 12:423–428. https://doi.org/10.1029/98WR01861

Chilton PJ, Foster SSD (1995) Hydrogeological characteristics and water-supply potential of basement aquifers in tropical Africa. Hydrogeol J 3:3–49. https://doi.org/10.1007/s100400050061

Chilton PJ, Smith-Carington AK (1984) Characteristics of the weathered basement aquifer in Malawi in relation to rural water supplies. In: Proc. Challenges Afr Hydrol Water Resour Symp, IAH Series Publ 144, IAH, Goring, UK, pp 15–23

Cho M, Ha KM, Choi Y-S, Kee W-S, Lachassagne P, Wyns R (2003) Relationship between the permeability of hard-rock and their weathered cover based on geological and hydrogeological observation in South Korea. In: IAH Conference on groundwater in fractured rocks, Prague, 15–19 September 2003

Compaore G, Lachassagne P, Pointet T, Trabi Y (1997) Evaluation du stock d'eau des altérites: expérimentation sur le site granitique de Sanon (Burkina Faso) [Assessment of the alterites water stock: experimentation on the granite site of Sanon (Burkina Faso)]. Rabat IASH conference, Publ. 241. IASH, Atlanta, GA, pp 37–46

Courtois N, Lachassagne P, Wyns R, Blanchin R, Bougaïre FD, Some S, Tapsoba A (2010) Large-scale mapping of hard-rock aquifer properties applied to Burkina Faso. Ground Water 48:269–283. https://doi.org/10.1111/j.1745-6584.2009.00620.x

Davis SN, Turk LJ (1964) Optimum depth of wells in crystalline rocks. Ground Water 2:6–11. https://doi.org/10.1111/j.1745-6584.1964.tb01750.x

Detay M, Poyet P, Emsellem Y, Bernardi A, Aubrac G (1989) Development of the saprolite reservoir and its state of saturation: influence on the hydrodynamic characteristics of drillings in crystalline basement (in French). C R Acad Sci Paris II 309:429–436

Dewandel, B, Maréchal JC, Bour O, Ladouche B, Ahmed S, Chandra S, Pauwels H (2012) Upscaling and regionalizing hydraulic conductivity and effective porosity at watershed scale in deeply weathered crystalline aquifers. J Hydrol 416–417:83–97. https://doi.org/10.1016/j.jhydrol.2011.11.038

Dewandel B, Lachassagne P, Wyns R, Maréchal JC, Krishnamurthy NS (2006) A generalized 3D geological ad hydrogeological conceptual model of granite aquifers controlled by single or multiphase weathering. J Hydrol 330:260–284. https://doi.org/10.1016/j.jhydrol.2006.03.026

Dong Y, Fu F, Yeh TJ, Wang Y, Zha Y, Wang L, Hao Y, (2019) Equivalence of Discrete Fracture Network and Porous Media Models by Hydraulic Tomography. Water Resour Res 55(4):3234–3247. https://doi.org/10.1029/2018WR024290

EC (2010) Report from the Commission in accordance with Article 3.7 of the Groundwater Directive 2006/118/EC on the establishment of groundwater threshold values. 5.3.2010 C 1096 final, European Commission, Brussels, 10 pp

Espinha Marques J, Samper J, Pisani B, Alvares D, Carvalho JM, Chaminé HI, Marques JM, Vieira GT, Mora C, Sodré Borges F (2010) Evaluation of water resources in a high-mountain basin in Serra da Estrela, central Portugal, using a semi-distributed hydrological model. Environ Earth Sci 62(6):1219–1234. https://doi.org/10.1007/s12665-010-0610-7

Espinha Marques J, Marques JM, Chaminé HI, Carreira PM, Fonseca PE, Monteiro Santos FA, Moura R, Samper J, Pisani B, Teixeira J, Carvalho JM, Rocha F, Borges FS (2013) Conceptualizing a mountain hydrogeologic system by using an integrated groundwater assessment (Serra da Estrela, central Portugal): a review. Geosci J 17(3):371–386. https://doi.org/10.1007/s12303-013-0019-x

Eyser (2012a) Estudio de la explotación en alta del abastecimiento al Baixo Miño, Augas de Galicia Technnical Report [Study of the exploitation of the supply in the Baixo Miño, Aguas de Galicia Technical Report]. Xunta de Galicia, A Coruña, Spain

Eyser (2012b), Informe acerca de la captación de manantiales para abastecer al depósito de A Riña en Oia, Augas de Galicia Technnical Report [Report on the collection of springs to supply the A Riña reservoir in Oia, Aguas de Galicia Technnical Report]. Xunta de Galicia, A Coruña, Spain

Fox RC, Hohmann GW, Killpack TJ, Rijo L (1980) Topographic effects in resistivity and induced polarization surveys. Geophys 45:75–93. https://doi.org/10.1190/1.1441041

Guihéneuf N, Boisson A, Bour O, Dewandel PJ, Dausse A, Viossanges M, Chandra S, Ahmed S, Maréchal JC (2014) Groundwater flows in weathered crystalline rocks: impact of piezometric variations and depth-dependent fracture connectivity. J Hydrol 511:320–334. https://doi.org/10.1016/j.jhydrol.2014.01.061

Gurtz J, Zappa M, Jasper K, Lang H, Verbunt M, Badoux A, Vitvar T (2003) A comparative study in modelling runoff and its components in two mountainous catchments. Hydrol Process 17:297–311. https://doi.org/10.1002/hyp.1125

Houston JFT, Lewis RT (1988) The Victoria Province drought relief project, II: borehole yield relationships. Ground Water 26(4):418–426. https://doi.org/10.1111/j.1745-6584.1988.tb00407.x

Howard KWF, Hughes M, Charlesworth DL, Ngobi G (1992) Hydrogeologic evaluation of fracture permeability in crystalline basement aquifers of Uganda. Hydrogeol J 1:55–65. https://doi.org/10.1007/S100400050029

Kottek M, Grieser J, Beck C, Rudolf B, Rubel F (2006) World map of the Köppen-Geiger climate classification updated. Meteorol Z 15(3):259–263

Krásný J (1997) Transmissivity and permeability distribution in hard rock environment: a regional approach. Hard Rock Hydrosystems (Proceedings of Rabat Symposium S2, May 1997). IAHS Pub. no. 241, pp 81–90

Krásný J (2002) Quantitative hardrock hydrogeology in a regional scale. Norges Geol Unders Bull 439:7–14

Krásný J, Sharp J (2007) Hydrogeology of fractured rocks from particular fractures to regional approaches: state-of-the-art and future challenge. In: Krásný J, Sharp J (eds) Groundwater in fractured rocks. IAH Selected Papers, vol 9. Taylor and Francis, London, pp 1–30

Lachassagne P, Wyns R, Bérad P, Bruel T, Chéry L, Coutand T, Desprats JF, Le Strat P (2001) Exploitation of high-yield in hard-rock aquifers: downscaling methodology combining GIS and multicriteria analysis to delineate field prospecting zones. Ground Water 41:333–341. https://doi.org/10.1111/j.1745-6584.2001.tb02345.x

Lee C-H, Farmer I (1993) Fluid Flow in Discontinuous Rocks, Chapman & Hall, London

Long JCS, Remer JS, Wilson CR, Witherspoon PA (1982) Porous media equivalents for networks of discontinuous fractures. Water Resour Res 18 (3):645–658. https://doi.org/10.1029/WR018i003p00645

Lu C, Samper J, Fritz B, Clement A, Montenegro L (2011) Interactions of corrosion products and bentonite: an extended multicomponent reactive transport model. Phys Chem Earth Parts A/B/C 36:1661–1668. https://doi.org/10.1016/j.pce.2011.07.013

Lu D-B, Zhou Q-Y, Junejo SA, Xiao AL (2015) A systematic study of topography effect of ERT based on 3-D modeling and inversion. Pure Appl Geophys 172:1531–1546. https://doi.org/10.1007/s00024-014-1015-4

Lubczynski MW, Gurwin J (2005) Integration of various data sources for transient groundwater modeling with spatio-temporally variable fluxes: Sardon study case, Spain. J Hydrol 306:71–96. https://doi.org/10.1016/j.jhydrol.2004.08.038

Maréchal JC, Dewandel B, Subrahmanyam K (2004) Use of hydraulic tests at different scales to characterize fracture network properties in the weathered-fractured layer of a hard rock aquifer. Water Resour Res 40:W11508. https://doi.org/10.1029/2004WR003137

Maréchal JC, Dewandel B, Ahmed S, Galeazzi L, Zaidi FK (2006) Combined estimation of specific yield and natural recharge in a semi-arid groundwater basin with irrigated agriculture. J Hydrol 329:281–293. https://doi.org/10.1016/j.jhydrol.2006.02.022

McFarlane MJ (1991) Some sedimentary aspects of lateritic weathering profile development in the major bioclimatic zones of tropical Africa. J Afr Earth Sci 12:267–282. https://doi.org/10.1016/0899-5362(91)90076-B

Molinero J, Samper J, Zhang G, Yang C (2004) Biogeochemical reactive transport model of the redox zone experiment of the Äspö Hard Rock Laboratory in Sweden. Nucl Technol 148:151–165

Nahon D, Tardy Y (1992) The ferruginous laterites. In: Butt CRM, Zeegers H (Eds) Regolith exploration geochemistry in tropical and sub-tropical terrains. Handb Explor Geochem 4, Elsevier, Amsterdam, pp. 41–55

Naves A, Samper J, Mon A, Pisani B, Montenegro L, Martins Carvalho J (2019) Demonstrative actions of spring restoration and groundwater protection in rural areas of Abegondo (Galicia, Spain). Sustain Water Resour Manag 5:175–186. https://doi.org/10.1007/s40899-017-0169-5

Oliva P, Viers J, Dupre B (2003) Chemical weathering in granitic environments. Chem Geol 202:225–256. https://doi.org/10.1016/j.chemgeo.2002.08.001

Peel MC, Finlayson BL, McMahon TA (2007) Updated world map of the Köppen-Geiger climate classification. Hydrol Earth Syst Sci 11:1633–1644. https://doi.org/10.5194/hess-11-1633-2007

Pérez-Alberti A, Trenhaile AS (2014) An initial evaluation of drone-based monitoring of boulder beaches in Galicia, north-western Spain. Earth Surf Process Landf 40:105–111. https://doi.org/10.1002/esp.3654

Pickens JF, Grisak GE, Avis JD, Belanger DW, Thury M (1987) Analyses and interpretation of borehole hydraulic tests in deep boreholes: principles model development, and applications. Water Resour Res 23:1341–1375. https://doi.org/10.1029/WR023i007p01341

Pisani B, Samper J, Espinha-Marques J (2019) Climate change impact on groundwater resources of Serra da Estrela mountain region in central Portugal. Sustain Water Resour Manag 5:289–304. https://doi.org/10.1007/s40899-017-0129-0

Pliego D, Corretge LG (1978) Geologic map of Spain (MAGNA), scale 1:50.000, sheet: Oya. Instituto Geológico y Minero de España (IGME), Madrid

Pliego D, Rubio J, Abril J, Corretge LG (1978) Geologic map of Spain (MAGNA), scale 1:50.000, sheet: Tuy. Instituto Geológico y Minero de España (IGME), Madrid

Rushton KR, Weller J (1985) Response to pumping test of a weathered-fractured granite aquifer. J Hydrol 80:299–309. https://doi.org/10.1016/0022-1694(85)90123-4

Samper J, Huguet L, Ares J, García Vera MA (1999) Manual del usuario del programa VISUAL BALAN v1.0: código interactivo Para la realización de balances hidrológicos y la estimación de la recarga [User manual of the program VISUAL BALAN v1.0: a user-friendly code to compute water balances and assess the aquifer recharge]. ENRESA 05/99, ENRESA, Madrid, 134 pp

Samper J, García Vera MA, Pisani B, Varela A, Losada JA, Alvares D, Espinha Marques J (2007) Using hydrological models and geographic information systems for water resources evaluation: GIS-VISUAL-BALAN and its application to Atlantic basins in Spain (Valiñas) and Portugal (Serra da Estrela). In: Lobo Ferreira JP, Vieira JMP (eds) Water in Celtic countries: quantity, quality and climate variability. IAHS Publ. 310, IAHS, Wallingford, UK, pp 259–266

Samper J, Xu T, Yang C (2009) A sequential partly iterative approach for multicomponent reactive transport with CORE^{2D}. Comput Geosci 13:301–316. https://doi.org/10.1007/s10596-008-9119-5

Samper J, Yang C, Zheng L, Montenegro L, Xu T, Dai Z, Zhang G, Lu C, Moreira S (2012) CORE^{2D} V4: a code for water flow, heat and solute transport, geochemical reactions, and microbial processes. In: Groundwater reactive transport models. Bentham Science, pp 160–185. https://doi.org/10.2174/978160805306311201010160

Samper J, Pisani B, Espinha Marques J (2015a) Hydrological models of interflow in three Iberian mountain basins. Environ Earth Sci 73:2645–2656. https://doi.org/10.1007/s12665-014-3676-9

Samper J, Li Y, Pisani B (2015b) An evaluation of climate change impacts on groundwater flow in the La Plana de la Galera and Tortosa alluvial aquifers (Spain). Environ Earth Sci 73:2595–2608. https://doi.org/10.1007/s12665-014-3734-3

Selroos J-O, Walker DD, Ström A, Gylling B, Follind S (2002) Comparison of alternative modelling approaches for groundwater flow in fractured rock. J Hydrol 257:174–188. https://doi.org/10.1016/S0022-1694(01)00551-0

Stigter TY, Nunes JP, Pisani B, Fakir Y, Hugman R, Li Y, Tomé S, Ribeiro L, Samper J, Oliveira R, Monteiro JP, Silva A, Tavares PCF, Shapouri M, Cancela da Fonseca L, Himer E (2014) Comparative assessment of climate change impacts on coastal groundwater resources and dependent ecosystems in the Mediterranean. Reg Environ Chang 14(Suppl 1):S41–S56. https://doi.org/10.1007/s10113-012-0377-3

Taylor R, Howard K (1998) Post-Paleozoic evolution of weathered land surfaces in Uganda by tectonically controlled deep weathering and stripping. Geomorphology 25:173–192

Taylor R, Howard K (2000) A tectono-geomorphic model of hydrogeology of deeply weathered crystalline rock: evidence from Uganda. Hydrogeol J 8:279–294. https://doi.org/10.1007/s100400000069

Thomas MF (1994) Geomorphology in the tropics. Wiley, New York

Walker DD, Gylling B, Strom A, Selroos JO (2001) Hydrogeological studies for nuclear-waste disposal in Sweden. Hydrogeol J 9:419–431. https://doi.org/10.1007/s100400100156

Wrigth EP (1992) The hydrogeology of crystalline basement aquifers in Africa. In: Wrigth EP, Burgess WG (eds) Hydrogeology of crystalline basement aquifers in Africa. Geol Soc Lond Spec Publ 66:1–27

Wu Y, Xu Y (2005) Snow impact on groundwater recharge in Table Mountain Group aquifer systems with a case study of the Kommissiekraal River catchment South Africa. Water SA 31:275–282. https://doi.org/10.4314/wsa.v31i3.5207

Wyns RJ, Gourry JC, Baltassat JM, Lebert F (1999) Caractérisation multiparamètres des horizons de subsurface (0–100 m) en contexte de socle altéré [Multiparameter characterization of subsurface horizons (0–100 m) in an altered basement context]. In: 2ème Colloque GEOFCAN, Orléans, France, BRGM, Orléans, France, pp 105–110

Wyns RJ, Quesnel F, Simon-Coinçon R, Guillocheau F, Lacquement F (2003) Major weathering in France related to litospheric deformation. Géol France 2003(1):79–87

Wyns RJ, Baltassat M, Lachassagne P, Legchenko A, Vairon J, Mathieu F (2004) Application of SNMR soundings for groundwater reserves mapping in weathered basement rocks (Brittany, France). Bull Soc Géol Fr 175:21–34